2010

# A Steam Expander for a Waste Heat Recovery Cycle

Hyan Jin Kim
*University of Incheon*

Hyun Jae Kim
*University of Incheon*

You Chan Kim
*University of Incheon*

# A Steam Expander for a Waste Heat Recovery Cycle

Hyun Jin Kim[1]*, Hyun Jae Kim[2], You Chan Kim[3]

University of Incheon, Dept. of Mechanical Engineering
12-1 Yeonsu-gu, Songdo-dong, Incheon, Korea
[1] E-mail: kimhj@incheon.ac.kr,
[2] E-mail: soricook@naver.com
[3] E-mail: youchan84@naver.com

## ABSTRACT

A steam expander has been studied for its usability as a power conversion device in a Rankine cycle, which can be used for on-site power generation or waste heat recovery. Design of a swash plate type expander has been practiced and its performance has been estimated. With the steam pressure and temperature of 3.5MPa and 300$^{o}$C at the expander inlet, respectively, it was calculated that the expander produced the shaft power output of about 2.88 kW from the steam heat source of 25kW. The expander output increased linearly with increasing the steam heat amount. For a given steam heat amount, the expander power increased with increasing the inlet steam temperature and it was not affected much by the inlet steam pressure. The expander efficiency was more or less constant at around 75%, regardless of the steam condition at the expander inlet.

## 1. INTRODUCTION

Recently, while multilateral measures are devised to reduce carbon dioxide emissions and reduce the use of fossil fuel which is expected to be exhausted soon, great attention is also being paid to energy recycles including waste heat recovery. Various cycles for as combined space heating and power, combined air conditioning and power or simply power generation from various types of heat sources have been suggested. Combustion heat, solar energy and other forms of waste heat can be used as heat source for power conversion cycles. Diego *et al*. (2006) carried out a theoretical analysis of waste heat recovery from an internal combustion engine. Under the concept of new recycled energy, the electricity and room heating/cooling energy needed in buildings without procuring energy from the outside like the case of net zero building are being attempted (Smith, 2007). Saitoh *et al*. (2007) studied solar organic Rankine cycle. Total thermal efficiency of their system was 7% for power generation. A case of a steam Rankine cycle for collecting car exhaustion gas waste heat to enhance car fuel efficiency by at least 13% was reported (Endo, 2007). Depending on the capacity and operating conditions of heat recovering cycles, the working fluid is selected and it is determined whether to use turbines or positive displacement type expanders.

In this study, a swash plate type steam expander that can be applied to steam Rankine cycles in order to convert the heat energy of steam into axle power will be designed and the performance of the designed steam expander will be estimated.

## 2. RANKINE CYCLE AND DESIGN OPERATING CONDITIONS

Figure 1(a) and (b) show a steam cycle with an expander for shaft power extraction and a corresponding T-s line diagram of the Rankine cycle, respectively. As the heat from a combustion engine exhaust gas is delivered to the water passing the evaporator (②→③), the water becomes high temperature and high pressure steam when it arrives at the outlet of the evaporator. This high temperature and high pressure steam passes through the expander (③→④) to generate axle power and then goes through the condenser (④→①) and is pumped at a high pressure in the water.

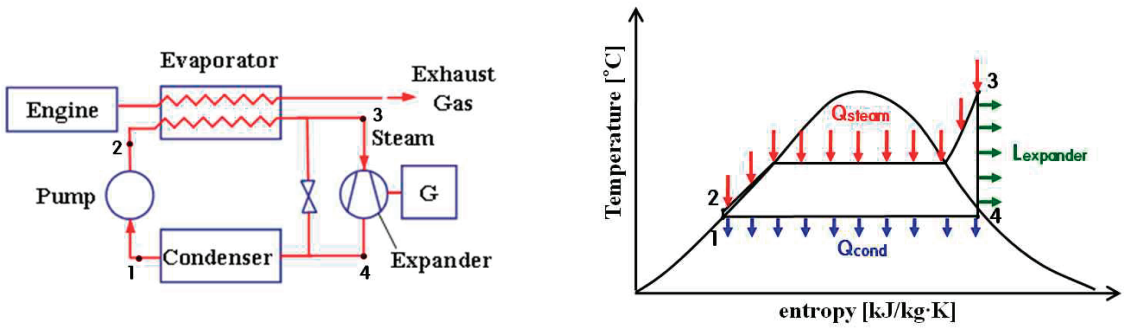


(a) (b)

Figure 1: Exhaust gas heat recovery system: (a) Steam cycle with expander as a power converter , (b) T-s diagram

supply pump (①→②) to go back to the evaporator. Here, the ideal Rankine cycle efficiency $\eta_{R,i}$ and the expander efficiency $\eta_e$ can be defined as equations (1) and (2), respectively

$$\eta_{R,i} = \frac{(h_3 - h_4) - (h_2 - h_1)}{h_3 - h_2} \tag{1}$$

$$\eta_e = \frac{L_s}{\dot{m}_s (h_3 - h_4)} \tag{2}$$

If the actual efficiency of the Rankine cycle is defined as the ratio of the shaft power ($L_s$) of the expander to the heat energy ($Q_{steam}$) supplied to the water, it is $(h_2–h_1)<<(h_3-h_4)$ and thus the actual efficiency of the Rankine cycle becomes equation (3).

$$\eta_R = \frac{L_s}{Q_{steam}} = \frac{\dot{m}_s (h_3 - h_4)}{Q_{steam}} \frac{L_s}{\dot{m}_s (h_3 - h_4)} \approx \eta_{R,i} \eta_e \tag{3}$$

Considering the pressure resistance and heat expansion property of the expander structure, a steam pressure $P_3$=3.5Mpa and temperature $t_3$=300°C at the inlet of the expander will be used as design operating conditions. Expander outlet conditions depend on the expansion ratio of the expander and if a swash plate type expander structure is adopted, an expansion ratio of around 10 can be obtained. In this case, the expander outlet conditions will be $P_4$=0.35Mpa and $t_4$=138°C and the steam will be in a two phase state with an approximate mass fraction $x_4$=0.9.

## 3. SWASH PLATE TYPE STEAM EXPANDER DESIGN

### 3.1 Expansion ratio and expansion commencing angle

If the crank angle and the piston position when the piston is at the top dead center are set to θ=0° and x=0, respectively, the piston position and the volume in the cylinder at a crank angle of θ will be as equation (4).

$$x = R_{sw} \tan\delta (1 - \cos\theta), V_c = A_p x + V_0 \tag{4}$$

Here, $A_p=\pi/4d_c^2$ is the cross section area of the piston, $V_0$ is the clearance volume, $R_{sw}$ is the radius of the swash plate and δ is the inclination angle of the swash plate. In this case, the piston displacement volume becomes $V_p=A_p$ $(2R_{sw}\tan\delta)$. In this design, considering the path of rotor valves etc, the volume ratio of the gap was determined as $\varepsilon=V_0/V_p=0.05$ and the expansion commencement angle as θ= 40.5°. In this case, the expansion ratio

becomes 10.5.

### 3.2 Steam flow rate and displacement volume

Relationships between the steam flow rate $m_s$ and the expander output $L_s$, and the expander displacement $V_{th}$ are given by equations (5) and (6) respectively.

$$L_s = \eta_e \dot{m}_s (h_3 - h_4) \tag{5}$$

$$V_{th} = \frac{\eta_e \dot{m}_s}{\rho_4 (N/60)} \tag{6}$$

If the overall efficiency and the volume efficiency of the expander are assumed as $\eta_e = 0.75$ and $\eta_v = 0.9$ and its rated driving speed is determined as N=1200 rpm, the steam flow rate and the expander displacement necessary to generate an expander power output of 3kW under the design operating conditions established earlier become $\dot{m}_s$=0.0088[kg/s] and $V_{th}$=208[cc], respectively.

### 3.3 Determination of major expander dimensions

To minimize leaks through the gap between the piston and the cylinder, piston rings should be applied. Since the temperature of the inhaled steam is as high as 300 $^oC$ , it is desirable to use existing commercialized piston rings for small engines and the smallest diameter of currently available small engine pistons is 30.2mm of pistons used on engines for grass cutters. Therefore, the diameter of pistons is fixed as $d_c$=30.2[mm]. If the number of cylinders is determined as $n_c$=8 considering the structure of inhaling valve ports and the continuity of steam inflows, the stroke necessary to make the given displacement is 36.4mm. If the router and swash plate are designed reflecting appropriate distances between cylinders necessary to secure structural stability and considering the mechanical stability and mobility of the swash plate, the effective diameter and inclination angle become $R_{sw}$=50[mm] and $\delta$=20$^o$ respectively. Figure 2 is a cross-section diagram of the swash plate type expander designed as such.

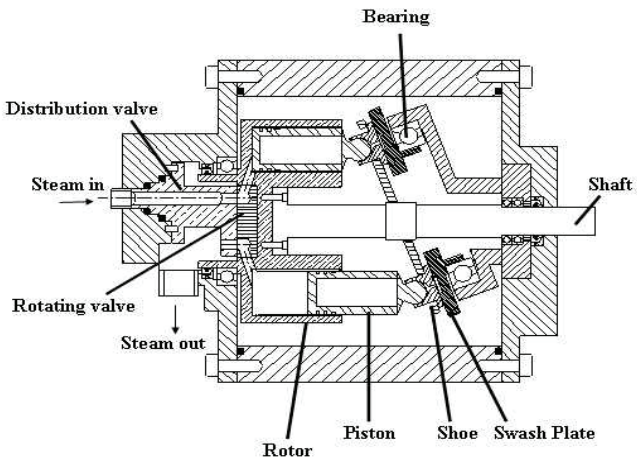


Figure 2: Swash plate type expander

## 4. PERFORMANCE ANALYSIS OF THE EXPANDER

### 4.1 Pressure calculation

Assuming the process of steam expansion as an isentropic process, P, the pressure in the cylinder is the function of density $\rho$ and it can be expressed by equation (7) and can be obtained from the values of the properties of steam.

$$P = P(\rho; s = s_0) \tag{7}$$

The density of steam is $\rho=M/V_c$ and it is obtained from the mass and volume in the cylinder and the mass in the cylinder is obtained considering the flow rates of the mass flowing into and flowing out of the cylinder and leaks as equation (8).

$$M = M_0 + \int (\dot{m}_v - \dot{m}_l) dt \tag{8}$$

In the two-phase region, the pressure can be obtained if steam vapor fraction $x_g$ is known along the isentropic line as shown in equation (9).

$$P = P(x_g; s = s_0) \tag{9}$$

Steam vapor fraction $x_4$ is determined as the value that makes the sum of the volumes occupied by vapor state steam and liquid state steam respectively become the volume of the cylinder as shown in equation (10).

$$V_c = (\frac{x_g}{\rho_g} + \frac{1 - x_g}{\rho_l}) M \tag{10}$$

However, the saturated densities of vapor state and liquid state $\rho_4$ and $\rho_1$ can be obtained only after knowing pressure P and thus eventually, equations (9) and (10) should be solved simultaneously.

### 4.2 Calculation of piston and rotor reactions

Figure 3 shows the forces applied to the piston and the reactions acting on the rotor. The balances of the forces and moments on the piston and the rotor are obtained as in equations (11) - (14).

$$F_{1,i} = F_{2,i} + F_{c,i} \tan\delta \tag{11}$$

$$(l_c - x_i) F_{2,i} = (l_p + x_i - l_c) F_c \tan\delta \tag{12}$$

$$R_1 + \sum_{i=1}^{8} F_{2,i} + R_2 - \sum_{i=1}^{8} F_{1,i} = 0 \tag{13}$$

$$l_{mj1} R_1 + (l_c - x_i) \sum_{i=1}^{8} F_{2,i} - l_{mj2} R_2 = 0 \tag{14}$$

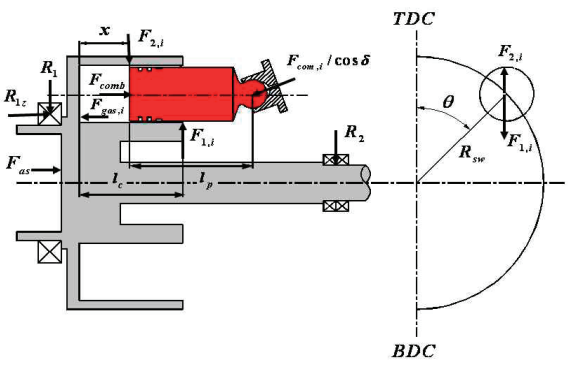


Figure 3: Force diagram on piston and rotor

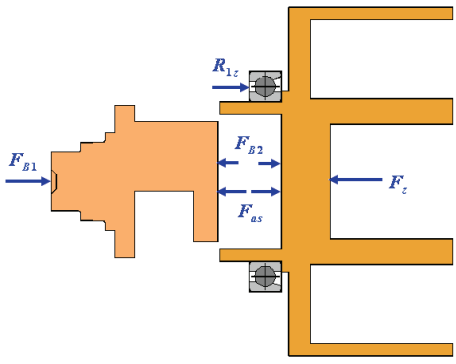


Figure 4: Force diagram on valve body

If the friction losses at the piston, the bearing supporting the rotor and the shaft, the bearing shoe caught by the piston ball, and the angular bearing supporting the swash plate are named $L_p$, $L_{R\text{-}S}$, $L_{shoe}$ and $L_{AB}$ , respectively, they can be represented by equations (15).

$$
\begin{aligned}
L_p &= \sum_{i=1}^{8} \mu_p \dot{x}_s (F_{1,i} + F_{2,i}) \\
L_{R-S} &= \mu_{BB}\omega(r_1\sqrt{R_1^{\,2} + R_2^{\,2}} + r_2 R_2) \\
L_{shoe} &= \sum_{i=1}^{8} \left|\dot{R}_{shoe}\right| \mu_{shoe} F_{com,i} / \cos\alpha \\
L_{AB} &= \sum_{i=1}^{8} \omega R_{AB} \mu_{AB} F_{com,i} / \cos\alpha \\
L_v &= r_v \omega \mu_v F_{B1}
\end{aligned}
\tag{15}
$$

Figure 4 shows the forces on the distribution valve and the rotor in the axial direction. $F_{B1}$ is the force due to the high pressure gas at the expander inlet tube, and $F_{B2}$ is the gas reaction from the rotor port openings.

## 5. CALCULATION RESULTS AND DISCUSSION

Figure 5 shows the P-V diagram obtained under the design operating conditions. The expansion power obtained from this expansion line diagram is $L_{PV}$=3060[W]. Since the theoretical expansion power is $L_{th}$= $\dot{m}_{th}(h_3-h_4)$=3859.6[W], the adiabatic expansion efficiency is $\eta_{ad}$=88.1%. Figure 6 shows various kinds of forces applied to each piston and rotor-shaft supporting bearings. The average values of individual components are as follows. $R_{1y}$=785.5[N], $R_{1z}$=2291.7[N], and $R_{2y}$=704.1[N], respectively. While $R_{1z}$, axial component of the angular bearing, being the difference between $F_z$ and $F_{B2}$, is the largest one among various bearing loads, largest friction loss occurs at the rotor frontal surface against the distribution valve body due to large friction coefficient of the boundary lubrication: $L_v$=71.6[W]. Average values of the other friction losses are $L_p$=24.7[W], $L_{R\text{-}S}$=36.7[W], $L_{shoe}$=14.2[W], and $L_{AB}$=28.7[W]. The total of mechanical friction losses is $L_{mech}$=175.9[W]. Therefore, the shaft power of the expander is $L_s$= $L_{PV}$–$L_{mech}$=2884[W] and the mechanical efficiency is $\eta_{mech}$=94.3%. The torque line diagram is shown in Figure 8.

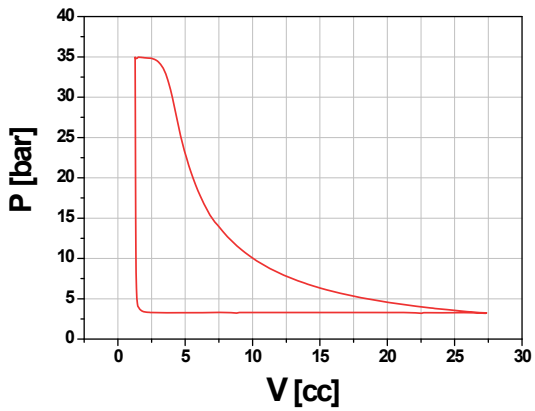


Figure 5: P-V diagram at $P_3$=35bar, $t_3$=300°C

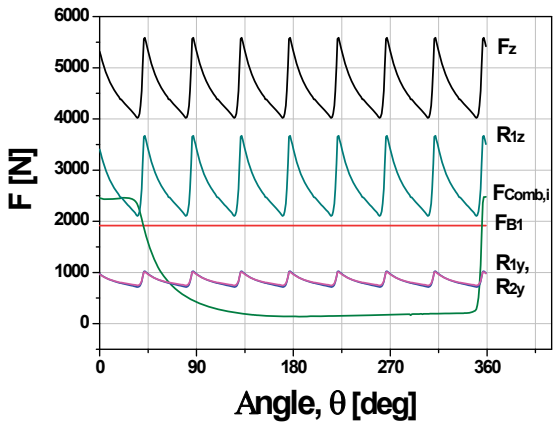


Figure 6: Various forces on piston and bearings

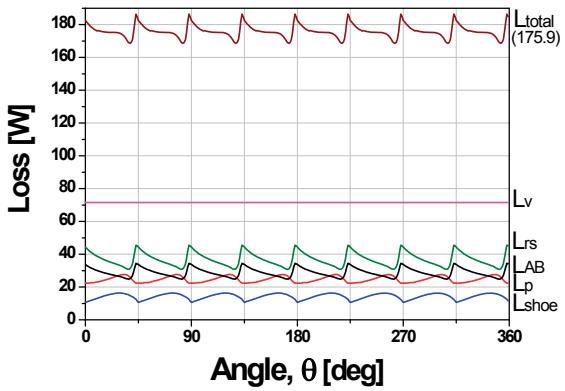


Figure 7: Mechanical losses

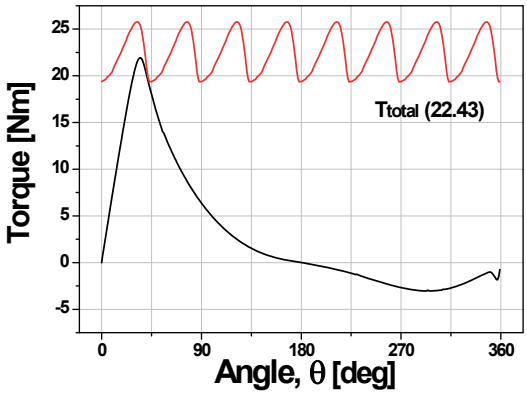


Figure 8: Torque variation

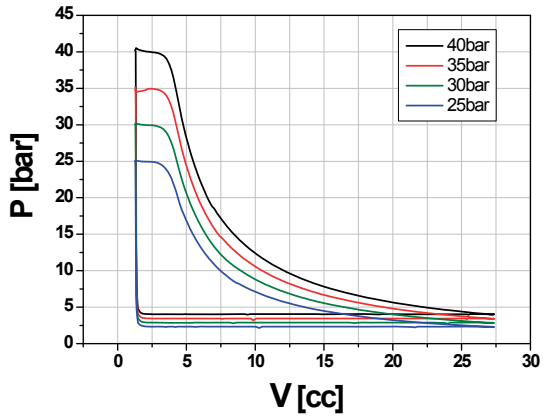


Figure 9: P-V diagrams at various inlet steam pressures: t3=300°C

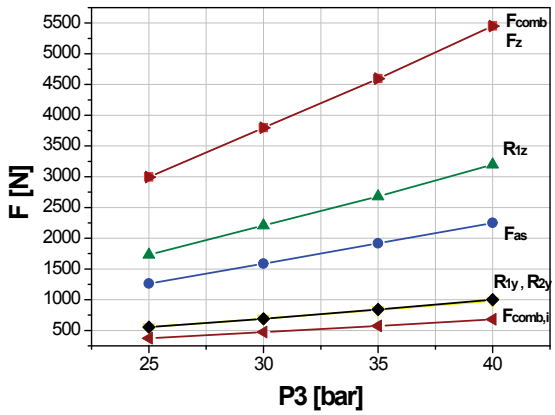


Figure 10: Force variation with inlet steam pressure: t3=300°C

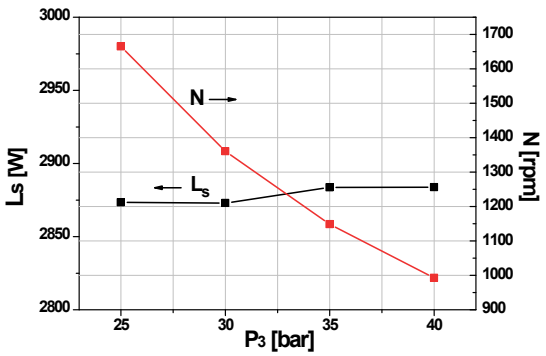


Figure 11: Effect of inlet steam pressure on the shaft power and speed: $t_3$=300°C

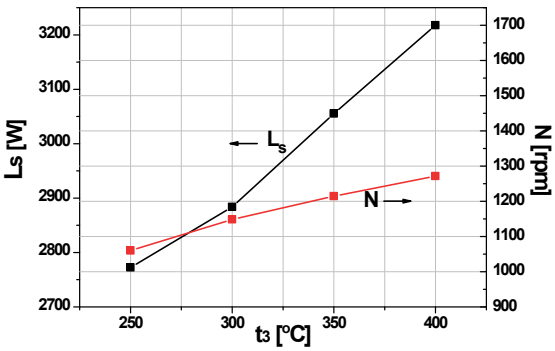


Figure 12: Effect of inlet steam temperature on the shaft power and speed: $P_3$=35bar

Effects of the inlet steam pressure $P_3$ on the P-V diagram and forces on the piston and bearings are respectively shown in Figures 9 and 10. Forces increase linearly with $P_3$. In Figure 11, with increasing $P_3$, the expander shaft power output shows only small increase, but the shaft speed decreases quite steeply. At lower $P_3$, expansion work per revolution becomes smaller but the shaft power does not change much due to increased shaft speed. Since the steam mass flow rate was held constant, the volume flow rate increases with lowering $P_3$, thus resulting in higher shaft speed. Effects of the inlet steam temperature $t_3$ on the expander performance are shown in Figure 12. With increasing $t_3$, both of the shaft power and speed increase, since the volume flow rate increases due to lowered steam density. Figure 13 shows that the expander efficiency is more or less constant over the covered range of the steam heat and that the expander power output changes linearly with steam heat.

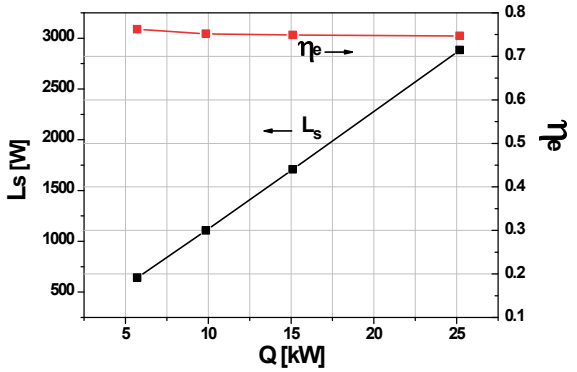


Figure 13 Expander shaft power and efficiency vs. steam heat

## 6. CONCLUSIONS

With regards to an expander applied to a steam Rankine cycle for the purpose of power generation from waste heat,

1) A basic design on a swash plate type expander with a shaft power output of 3kW grade was carried out.
2) The displacement of the designed expander is 208cc when the use of the existing piston ring for small engines is assumed. The built-in expansion ratio is 10 and it is designed to run at the speed of 1200rpm at the rated output.
3) It was calculated that an expander output of 3kW could be obtained from the steam energy of 25kW when the steam pressure and temperature at the expander inlet are $P_s$=35 bar and $t_3$=300$^o$C, respectively.
4) The adiabatic expansion efficiency was calculated to be $\eta_{ad}$=88.1%and the mechanical efficiency was calculated to be $\eta_{mech}$=94.3% and the overall efficiency of the expander becomes $\eta_e$=74.7% when the volumetric efficiency is $\eta_v$=90%.
5) The expander power output and the shaft speed increase with increasing the inlet steam temperature, but the inlet steam pressure does not affect much on the power output.

## NOMENCLATURE

| | | | |
|---|---|---|---|
| F | force | (N) | |
| h | enthalpy | (kJ/kg) | |
| L | power, power loss | (W) | |
| $\dot{m}$ | mass flow rate | (kg/s) | |
| N | shaft speed | (rpm) | |
| P | pressure | (Pa) | |
| Q | heat | (W) | |
| R | bearing force | (N) | |
| $R_{sw}$ | swash plate radius | (m) | |

**Subscripts**

| | |
|---|---|
| AB | angular bearing |
| e | expander |
| R-S | rotor-shaft |
| R | Rankine cycle |
| p | piston |
| s | shaft |
| shoe | shoe bearing |
| v | valve |

| | | | | |
|---|---|---|---|---|
| s | entropy | (kJ/kg) | **Greeks** | |
| t | temperature | ($^oC$) | δ | swash plate angle |
| V | volume | ($m^3$) | ε | clearance volume ratio |
| x | piston displacement, vapor fraction | (m, -) | η | efficiency |
| | | | ρ | desity |

## REFERENCES

Endo T., Kawajiri S., Kojima Y., Takahashi K., Baba T., lbaraki S., Takahashi T., Shinohara M., 2007, Study on Maximizing Exergy in Automotive Engines, *SAE International* Paper 2007-01-0257

Arias D., Shedd T., Jester R., 2006, Theoretical Analysis of Waste Heat Recovery from an Internal Combustion Engine in a Hybrid Vehicle, *SAE International* Paper 2006-01-1605

Saitoh, T., Yamada, N., and Wakashima, S., 2007, Solar Rankine cycle system using scroll expander, *Journal of Environment and Engineering*, vol. 2, no.4: p.708-719.

Smith, P., 2007, *Sustainability at the Cutting Edge*, Architectural Press, second edition.